

# A pilot study of macrophage responses to silk fibroin particles

Xidong Cui,<sup>1,2</sup> Jianchuan Wen,<sup>3</sup> Xia Zhao,<sup>2</sup> Xin Chen,<sup>3</sup> Zhengzhong Shao,<sup>3</sup> Jack J. Jiang<sup>1</sup>

<sup>1</sup>Department of Otolaryngology, Eye, Ear, Nose and Throat Hospital, Fudan University, Shanghai 200031, China

<sup>2</sup>Department of Otorhinolaryngology-Head and Neck Surgery, Huashan Hospital of Fudan University, Shanghai 200040, China

<sup>3</sup>Department of Macromolecular Science and the Laboratory of Advanced Materials, Fudan University, Shanghai 200433, China

Received 23 March 2012; revised 28 June 2012; accepted 5 September 2012

Published online 7 December 2012 in Wiley Online Library (wileyonlinelibrary.com). DOI: 10.1002/jbm.a.34444

**Abstract:** Silk fibroin (SF) shows promise for tissue engineering and other biomedical applications due to its excellent biocompatibility, unique biomechanical properties, and controllable biodegradability. The particulate form of SF materials may have many potential uses, including the use as a filler for tissue defects or as a controlled-release agent for drug delivery. However, many past *in vivo* and *in vitro* studies evaluating the biocompatibility and biodegradability of SF have involved bulk implants. It is essential to evaluate the inflammatory effects of SF particles before further use. In this study, two different sizes of SF particles were evaluated to assess their impact on the release of tumor necrosis factor (TNF)- $\alpha$ , interleukin (IL)-1 $\beta$ , and IL-6, in comparison with lipopolysaccharide positive control stimulation. The inflammatory processes were characterized using real-time reverse transcription polymerase chain reaction, enzyme-linked immunosorbent

assay, and light microscopy evaluations. The results indicated that small silk fibroin particles and large silk fibroin particles, in culture with RAW 264.7 murine macrophage cells for 24 h, caused up-regulation of mRNA coding for TNF- $\alpha$ , which indicated that both size of particles have potential inflammatory effects. There was a statistically significant increase in this up-regulation under small silk fibroin stimulation. However, the immunosorbent assay suggested that there was virtually no observed release of IL-1 $\beta$ , IL-6, or TNF- $\alpha$ , relative to the control group. The results suggest that SF particles of the chosen dimensions may have good biocompatibility in culture with RAW 264.7 murine macrophages. © 2012 Wiley Periodicals, Inc. *J Biomed Mater Res Part A*: 101A: 1511–1517, 2013.

**Key Words:** silk, fibroin, macrophage, biocompatibility, *in vitro*, inflammation, cytokine

**How to cite this article:** Cui X, Wen J, Zhao X, Chen X, Shao Z, Jiang JJ. 2013. A pilot study of macrophage responses to silk fibroin particles. *J Biomed Mater Res Part A* 2013;101A:1511–1517.

## INTRODUCTION

Silk fibroin (SF) shows promise for tissue engineering and other biomedical applications<sup>1–3</sup> due to its excellent biocompatibility, unique biomechanical properties, and controllable biodegradability. Such properties have attracted interest of investigators from biomedical fields and other related disciplines. SF is a versatile biomaterial that can be prepared in various forms and shapes, ranging from nanometer to centimeter scales. This versatility allows it to be utilized for a variety of purposes. Although the majority of SF application focuses on tissue engineering involving bone, cartilage, nerve, and blood vessel repair,<sup>4–8</sup> there is increased interest regarding the role of particulate SF in drug delivery mechanisms.<sup>9–12</sup> The particulate form of SF materials, as injectable fillers, may also have potential use for synthetic repair of tissue defects such as glottic insufficiency caused by unilateral vocal fold paralysis.

However, most of the *in vivo* and *in vitro* studies observing biocompatibility and biodegradability of SF have dealt

primarily with bulk implants. It is likely that particulate implantation of the same materials may elicit significantly different inflammatory response, compared with bulk implantation.<sup>13,14</sup> Observation of implanted materials has suggested that the size, concentration, surface area, and volume dimensions of implanted particulate material play an important role in the tissue-cellular response.<sup>15–18</sup> Therefore, it is important that the inflammatory response elicited by particular SF biomaterials could be investigated prior to application on a broader scale.

Monocytes/macrophages serve as an effective study system, due to their active roles in the processes of inflammation and wound healing.<sup>19</sup> A variety of investigations have focused on the interactions between biomaterial particles and macrophages, and histological examinations have revealed that macrophages play a central role in the response to the particles.<sup>20–23</sup> For this reason, many *in vitro* studies have aimed at simulating an *in vivo* response through the examination of macrophages. More specifically,

**Correspondence to:** Jack J. Jiang; e-mail: jackjiang@gmail.com

Contract grant sponsor: National Natural Science Foundation of China; contract grant number: 81028004

Contract grant sponsor: Shanghai Science and Technology Committee; contract grant number: 1052nm03801

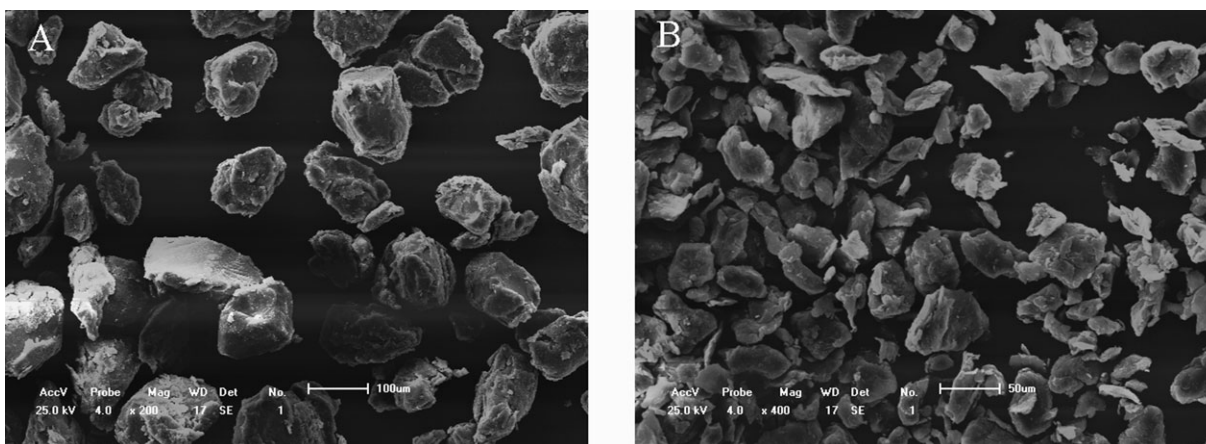


FIGURE 1. Scanning electron micrographs of fibroin particles: (A) SFL; (B) SFS.

macrophage cells have been employed extensively for *in vitro* studies to evaluate the inflammatory responses triggered by various biomaterials.<sup>14,24–26</sup> Many cytokines and interleukins, including tumor necrosis factor (TNF)- $\alpha$ , interleukin (IL)-6, and IL-1 $\beta$ , have been widely found in pseudomembranes of failed total hip arthroplasty cases, as well as in other *in vitro* studies.<sup>27–30</sup> These three cytokines, which are proinflammatory cytokines that recruit other inflammatory and immune cells, have been implicated as playing substantial roles in the inflammatory response.

In this investigation, we provide initial pilot results for an *in vitro* study of biocompatibility in SF particles. Two different sizes of SF particles were selected to investigate their role in stimulating the release of TNF- $\alpha$ , IL-1 $\beta$ , and IL-6, in comparison with lipopolysaccharide (LPS) positive control stimulation. The inflammatory processes were characterized using real-time reverse transcription polymerase chain reaction (RT-PCR), enzyme-linked immunosorbent assay (ELISA), and light microscopy evaluations.

## MATERIALS AND METHODS

### Preparation of SF particles

SF particles were prepared according to previously established methods.<sup>31,32</sup> *Bombyx mori* silk cocoons were degummed twice in 0.5% (w/w) aqueous NaHCO<sub>3</sub> solution at 95°C for 30 min. After being washed thoroughly with distilled water and then dried, the degummed silk was dissolved in 9.5M LiBr aqueous solution for about 1 h at 45°C with gentle stirring. After being filtered, the resulting fibroin solution was dialyzed against deionized water for 4 days at room temperature with a 14 kDa cutoff dialysis membrane to remove the salt. The dialyzed SF solution was centrifuged at 6000 rpm for 10 min. Then, the clarified solution in the supernatant was collected and concentrated by reverse dialysis against a 10% (w/v) polyethylene glycol (20,000 Da) to give a 20% (w/w) SF solution, following previously reported methods (China invention patent, application no. 03142201.2; public no. CN 1483866A).

SF solution was poured into polystyrene disks (5 cm  $\times$  5 cm) and dried in a fume hood for 2–3 days to form

0.5- to 1-mm-thick films. SF films were subsequently treated with 70% (v/v) ethanol for 24 hours to enhance the  $\beta$ -sheets structure in regenerated SF, which allows for further solidification. All films were stored in 70% (v/v) ethanol solution which served as a sterile environment.

Before experimental use, the films were thoroughly washed with distilled water to remove ethanol, then cut into small pieces and dried at 60°C in a thermostatic electric air-drying box (GZX-9070MBE; Shanghai Boxun Industry and Commerce Co., Ltd., Shanghai, China) for over 48 h. The fully dried SF pieces were mechanically grinded with a mixer mill (MM 400; Retsch Technology, Germany) to produce SF particles at 25 Hz for 8 min. The milled SF particles were sieved with a vibratory sieve shaker (AS200 control; Retsch Technology, Germany) to segregate particles into two appropriate size ranges: 10–45  $\mu$ m (small silk fibroin particles; SFS) and 45–125  $\mu$ m (large silk fibroin particles; SFL). The size and morphology of the particles were confirmed by scanning electron microscopy (SUPERSCAN SSX-550; Shimadzu, Japan) (Fig. 1).

All the SF particles were treated with 70% ethanol solution for at least 48 h to sterilize and remove bound endotoxins.<sup>33</sup> Particles were rinsed thoroughly with distilled water, then suspended and sonicated in sterile phosphate buffered saline (PBS) before use. All procedures were carried out with extreme care and performed under clean and sterile conditions (instruments, containers, etc.) to avoid any contamination.

### Macrophage culture

A RAW 264.7 murine macrophage cell line obtained from the Cell Bank of the Chinese Academy of Sciences (Shanghai, China) was used in this study. We selected this specific cell line because of their reproducibility and the ease of culturing that they permit. This is also one of the cell lines frequently used by other authors to evaluate particle responses.<sup>14,26</sup> The cells were expanded and maintained in 75 cm<sup>2</sup> cell culture flasks (Corning Glass Works, Corning, NY). They were suspended in Dulbecco's Modified Eagle Medium (DMEM, Sigma), containing 10% fetal bovine serum (FBS, Gibco), and

cultured in an incubator with a moist atmosphere consisting of 5% CO<sub>2</sub> to 95% air at 37°C. Media contained 100 U/mL of penicillin and 100 µg/mL of streptomycin.

After formation of the cell monolayer (80% cell confluence), the culture medium was carefully removed and the flasks were washed twice with PBS solution. An additional 15 mL of PBS was added to the flask, and the cells that remained on the flask surface were harvested with a cell scraper (Corning Glass Works).

The medium containing the cells was then pipetted and transferred to 20-mL sterile tubes, which were centrifuged at 1000 rpm for 10 min to separate the cells from the medium. After centrifugation, the supernatant was discarded and 10 mL of culture medium was added to each tube containing the cells. The total number of cells was counted in a hemocytometer, yielding a subcultivation ratio of 1:8. The surplus cells were preserved in complete growth medium supplemented with 5% (v/v) dimethylsulfoxide (DMSO, Sigma) in liquid nitrogen.

### Macrophage stimulation and assay

RAW 264.7 macrophages were seeded in 2.5 mL cell cultures in different wells of a 6-well plate, delivering approximately  $2 \times 10^5$  cells per well. The macrophage cells were plated for 24 h, washed with PBS, then subject to new culture media prior to stimulation.

Once prepared for experimental use, the cells were challenged with SFL particles (5 mg/well,  $n = 6$ ) and SFS particles (5 mg/well,  $n = 6$ ), respectively. For experimental purposes, the SFL replicates correspond to group A, whereas the SFS particles comprise group B. We chose an SF dosage of 5 mg/well, because at this dosage, the cells were thinly covered by the particles. Our results depict data gathered after 24 h incubations only, since previous studies have shown that the maximum cytokine production—by cultured macrophages in response to particles—occurs after 15–20 h of incubation.<sup>14,34</sup> And our preliminary experiment found that longer observation times without replacement of the culture media may result in over proliferation and death of the cells.

For our positive control ( $n = 6$ ; group C), LPS (Sigma, L6529) was added to the cells at a terminal concentration of 1 µg/mL. The negative control ( $n = 6$ ; group D) consisted of cells cultured in standard medium alone. All stimulations, with the exception of LPS positive controls, were carried out in the presence of 5 µg/mL Polymyxin B to inhibit any LPS contamination.<sup>14</sup>

Cells were examined using light microscopy in order to observe their morphology, which was assessed in terms of cell attachment to the plate. After exposure to the stimulation for 24 h, the supernatant of the cell culture media was collected and centrifuged to remove particulate matter. The solution was aliquoted and stored at -20°C for later evaluation of cytokine levels. The cells in each well were washed with PBS to remove the particles and the growth media, followed by the addition of 1 mL of TRIzol® Reagent (Invitrogen, Carlsbad, CA) in order to lyse the cells. We pipetted the cells up and down several times to homogenize the samples, and then stored them at -80°C to prepare them for mRNA extraction.

### Real-time RT-PCR assays of the stimulated macrophages

RNA was extracted from RAW 264.7 cells using TRIzol® Reagent, following the manufacturer's protocol. Quantity and purity of RNA were determined by absorbance values indicated on a spectrophotometer (BioMate 3S, Thermo Scientific) at 260 and 280 nm. For reverse transcription, 1.6 µg of RNA was reversely transcribed with Oligo (dT)<sub>18</sub> (Fermentas), and complementary DNA was amplified according to the manufacturer's instructions. Primers were designed and synthesized by Sangon Biotech Shanghai Co. Ltd, Shanghai, China. Real-time RT-PCR was performed to detect gene expression of IL-1β, IL-6, and TNF-α, using the ABI Prism 7500 (Applied Biosystems, Foster City, CA) real-time system in triplicate for all samples.

The forward and reverse primers for IL-1β are 5'-TGAAATGCCACCTTTTGACAG-3' and 5'-CCACAGCCACAATGAGTGATAC-3', respectively; for IL-6, forward primer 5'-ACAAAGCCAGAGTCCTTCAGAG-3' and reverse primer 5'-AAGATGAATTGGATGGTCTTG-3'; and for TNF-α, forward primer 5'-GCCTATGTCTCAGCCTCTTCTC-3' and reverse primer 5'-CACTTGGTGGTTTGTACGA-3'. The housekeeping gene, β-actin, was selected as a reference gene in order to control the intersample variation in RNA isolation and integrity. This was done by using a pair of primers: forward primer 5'-GAGACCTTCAACACCCCAGC-3' and reverse primer 5'-ATGTCACGCACGATTTCCC-3'. The amplification conditions were 95°C for 2 min followed by 40 cycles of 95°C for 20 s, 57.5°C for 30 s, and 72°C for 32 s. For each assay, 0.25 µM (terminal concentration) of both forward and reverse primers and approximately 32 ng of complementary DNA template were added to each reaction of the GoTaq qPCR Master Mix (Promega) for a total reaction volume of 20 µL.

At the end of each reaction, a cycle threshold (Ct) was manually setup at the level that reflected the best kinetic PCR parameters, followed by observation of melting curves and subsequent analysis. Ct is defined as the PCR cycle number during which an increase in fluorescence beyond a threshold occurs. Amplification products were quantified by comparison of experimental Ct levels. The expression data for each gene product were normalized against the Ct level of the β-actin housekeeping gene. The resulting transcript Ct levels are reported as mean relative changes ( $\pm$  range) compared to untreated controls. The  $\Delta\Delta$ Ct method of relative quantification was adapted and optimized to estimate the quality of the four genes previously indicated.

### Determination of macrophage cytokine release

Concentrations of IL-1β, IL-6, and TNF-α in the supernatants of the cell culture were quantified using ELISA kits (BioTNT, Shanghai, China) according to the manufacturer's protocol. These were ELISA kits that are murine specific. Cytokine concentration was calculated by comparison with standard curves of known values of recombinant murine IL-1β, IL-6, and TNF-α. Measurements of optical densities were performed with ELISA reader (DNM-9602; Beijing Prolong New Technology Co., Ltd., Beijing, China) at 450 nm wavelength. All samples and standards were processed in duplicate wells and the results were expressed in pictograms per

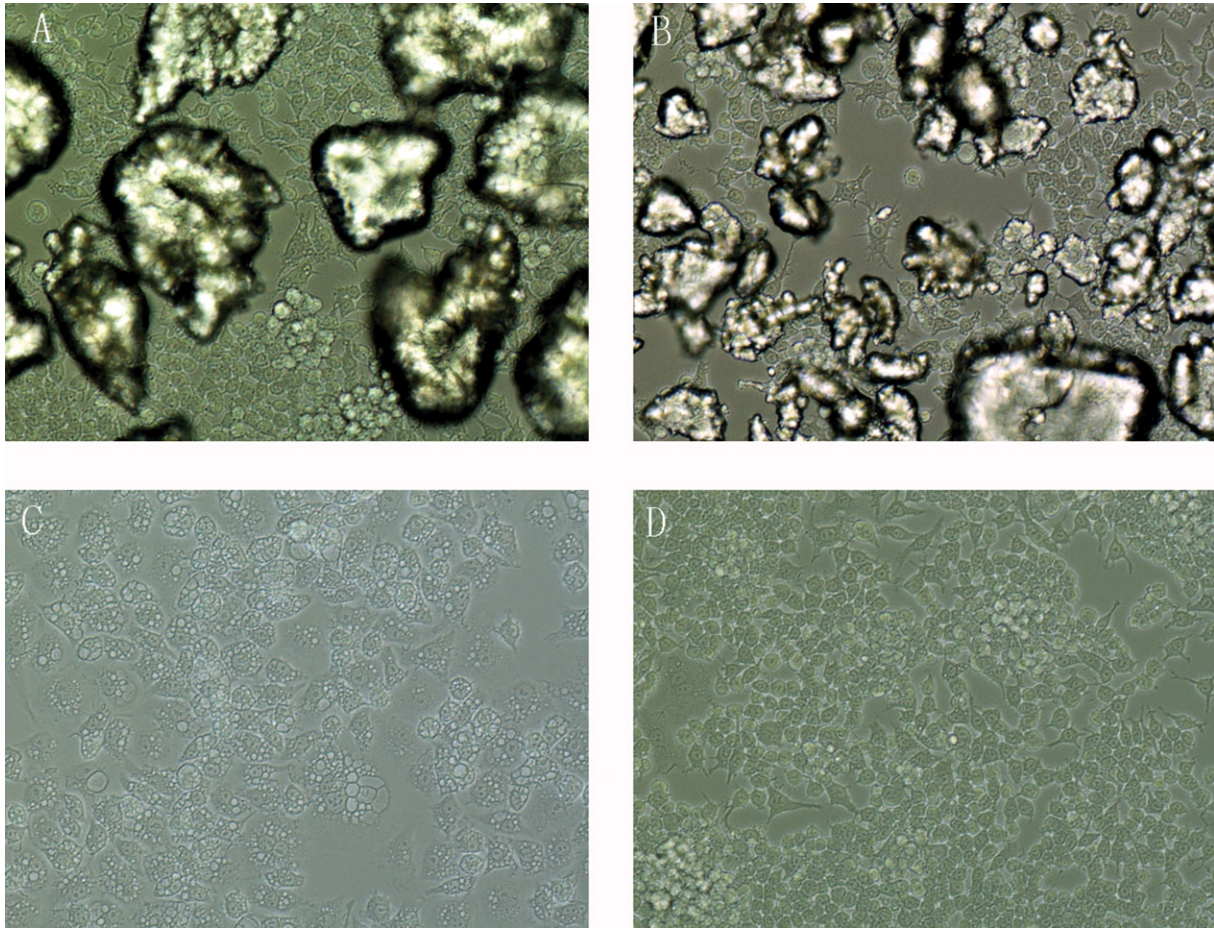


**FIGURE 2.** Light microscopy observation of Raw 264.7 cell activation, stimulated by SFL (A), SFS (B), LPS (C), and negative control (D),  $\times 200$ . [Color figure can be viewed in the online issue, which is available at [wileyonlinelibrary.com](http://wileyonlinelibrary.com).]

milliliter. The cytokines released in the blank control were subtracted from all other samples as a baseline.

### Statistical analysis

Statistical analysis was performed using a commercially available statistical software prism 5.0 (GraphPad Software Inc., San Diego, CA). All data were expressed as mean  $\pm$  standard deviation (SD) for  $n = 6$ . Statistics were produced using one-way analysis of variance (ANOVA) tests as well as Tukey's HSD post-hoc comparison test. The value of  $p < 0.05$  was considered statistically significant.

## RESULTS

### Light microscopy observations of RAW 264.7 cell activation

After stimulation for 24 h, the challenged macrophages were viewed under an inverted phase contrast microscope (Nikon Ti-E, Japan), showing activation of the cells. All three stimulated sample groups (SFL, SFS, and LPS) exhibited morphological changes, which included enlarged cell sizes, increased vacuolization, and the presence of pseudopod-like structures. The morphological changes of the RAW 264.7 cell line in groups A and B were almost the same, having slight enlargement and polymorphism of cell bodies, with a

few cells having bubble-like constitution in the plasma [Fig. 2(A) and (B)]. In group C, however, the similar morphological changes were dramatically characterized by alveolar macrophage changes [Fig. 2(C)]. In contrast, group D showed almost no changes of cell morphology except proliferation of the cells [Fig. 2(D)].

### Induction of mRNAs of IL-1 $\beta$ , IL-6, and TNF- $\alpha$ of the stimulated macrophages

The mRNA expression of proinflammatory cytokines IL-1 $\beta$ , IL-6, and TNF- $\alpha$  were evaluated by real-time RT-PCR (Fig. 3). LPS stimulation caused a marked increase in the expression of mRNAs indicative of IL-1 $\beta$ , IL-6, and TNF- $\alpha$  ( $p < 0.001$  vs. control). Despite this result, IL-1 $\beta$  and IL-6 mRNAs for the SFL and SFS stimulated groups were observed to be relatively similar to the control group ( $p > 0.05$ , respectively). However, macrophages stimulated by SFL and SFS both showed increased expression of TNF- $\alpha$ -suggestive mRNA when compared with the control cells ( $p < 0.001$ , respectively), but much less than the positive control ( $p < 0.001$ ). Furthermore, we observed higher levels of such mRNA in the SFS-stimulated group, compared with the SFL group ( $p < 0.001$ ). These results indicated that the SFS particles may have higher inflammatory-inducing nature.

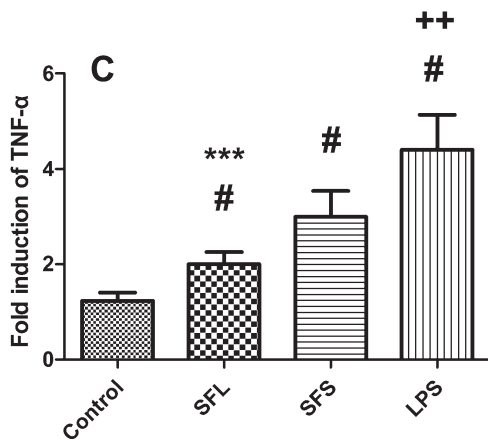
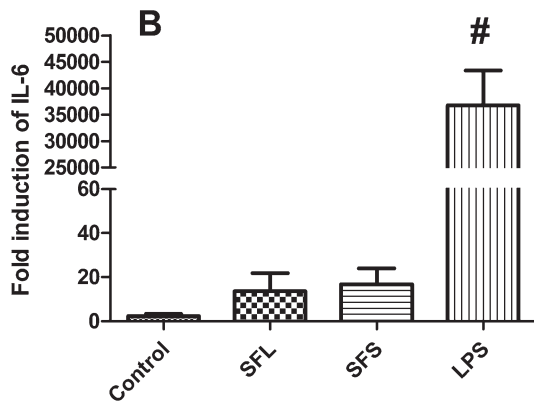
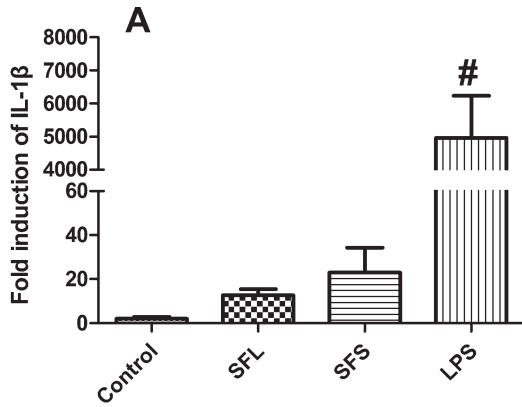


**FIGURE 3.** IL-1 $\beta$ , IL-6, and TNF- $\alpha$  expression of the stimulated macrophages. Each value in real-time RT-PCR graphs (A, B and C) represents the mean  $\pm$  SD of 6 wells of cells in each group. # $p < 0.001$  vs. control group; \*\*\* $p < 0.001$  vs. SFS group.

**Concentrations of IL-1 $\beta$ , IL-6, and TNF- $\alpha$  in the supernatants of the cell culture after stimulations**

We examined the pro-inflammatory IL-1 $\beta$ , IL-6, and TNF- $\alpha$  cytokines using ELISA. The stimulation of the macrophages with LPS for 24 h increased levels of all the three cytokines noticeably, compared with the other three groups ( $p < 0.001$ , respectively) [Fig. 4(A)–(C)]. In contrast, SFL and SFS administration at a concentration of 5 mg/well created no obvious difference in cytokine concentrations, compared

with the negative control cells ( $p > 0.05$ , respectively). Additionally, there was no significant difference between the particle populations with respect to expression and secretion of the cytokines being observed ( $p > 0.05$ ). These results suggest that neither SFL nor SFS will provoke inflammatory responses from RAW 264.7 macrophages.

**DISCUSSION**

The purpose of this investigation was to evaluate the immunostimulating properties of two different sizes of SF particles. Inflammatory response was gauged by morphological changes; production of IL-1 $\beta$ , IL-6, and TNF- $\alpha$  cytokines;

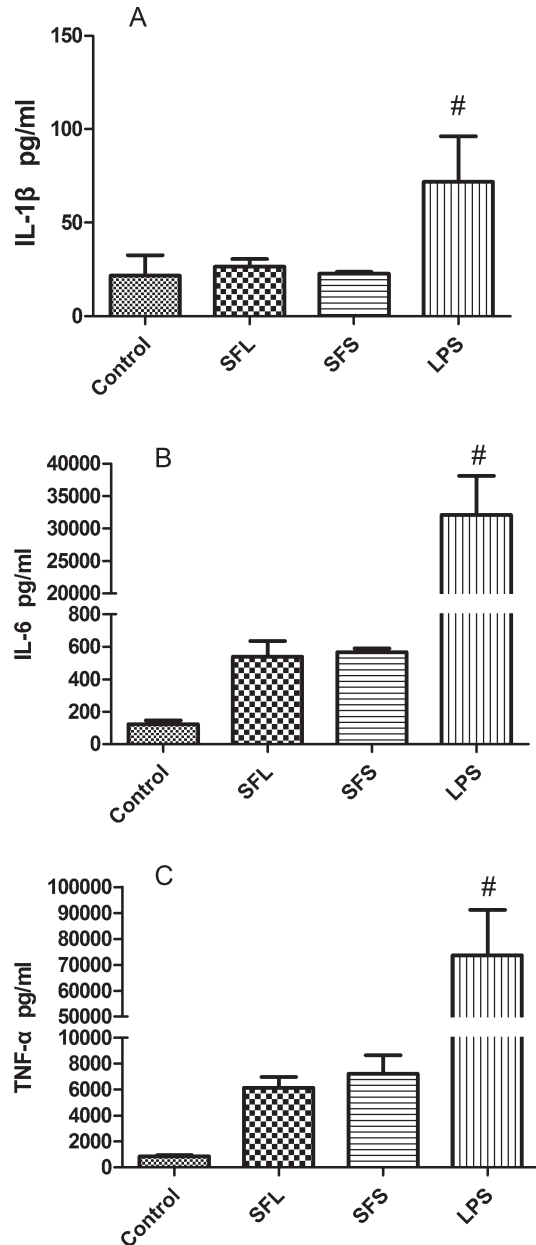


**FIGURE 4.** ELISA analysis of IL-1 $\beta$ , IL-6 and TNF- $\alpha$  secretion. Each value represents the mean  $\pm$  SD of 6 wells containing supernatants of the cell culture in each group. # $p < 0.001$  vs. control group.

and transcription of the matching mRNA by RAW264.7 macrophages, following exposure to these biomaterials.

We chose to assay for IL-1 $\beta$ , IL-6, and TNF- $\alpha$ , which are proinflammatory cytokines that recruit other inflammatory and immune cells; activating these compounds upon arrival at implant sites. These three cytokines are thus suggested to play a valuable role in the inflammatory response process, making them ideal indicators of such activity. Obviously, additional or other cytokines could have been measured, but we limited our selection to these three for our pilot study. These are also the three cytokines selected for evaluation by many other investigators as described in the Introduction section.

Noticeable presences of pseudopod-like structures and bubble-like constitution in the plasma were observed in macrophages responding to both SFL and SFS 24-h stimulation. However, there was a more pronounced response to LPS stimulation. Treatment with LPS caused morphological changes characterized by larger nuclei, prominent nucleoli and relatively prominent cytoplasm with increased granularity,<sup>35,36</sup> and enhanced secretion of TNF- $\alpha$  and other proinflammatory cytokines by macrophages as previously reported.<sup>37</sup> In this study, the functional consequence accompanied with these morphological changes in SFL and SFS groups is up-regulated transcription of TNF- $\alpha$  mRNA, which encode TNF- $\alpha$ , a pleiotropic molecule that plays a central role in inflammation. We observed higher expression of TNF- $\alpha$  mRNA with SFS stimulation compared with that in the SFL dose. With respect to translation of mRNA, although these were statistically insignificant, similar differences in TNF- $\alpha$  secretion also existed. The results indicated that both SFL and SFS have potential inflammatory activity and furthermore demonstrated that SFS may cause more inflammation.

There were no statistically significant differences observed between the SFS and SFL samples for the presence of either the IL-1 $\beta$  or IL-6 mRNAs, compared with the negative control (Fig. 3). Similarly, there were no significant differences in measured secretion levels for either of these corresponding cytokines (IL-1 $\beta$  or IL-6), when observing the SFS and SFL samples relative to the control (Fig. 4). These results suggest that TNF- $\alpha$  may be the most abundant inflammatory mediator resulting from stimulation by SF particles. A study by Kaplan and co-workers also observed that insoluble, irregularly shaped fibroin particles of approximately 10–200  $\mu$ m size induced significant TNF- $\alpha$  production<sup>14</sup> under an experimental setup similar to our SF particle. SF particles have certain anti-tumor activity effect through influence of innate and adaptive immune system,<sup>38</sup> which may be another possible reason inhibiting the overall expression of IL-1 $\beta$  and IL-6.

Previous studies have also demonstrated that particles smaller than 10  $\mu$ m could be phagocytosed by macrophages and produce subsequent tissue reactions through secretions of inflammatory cytokines.<sup>24,39</sup> In this study, the SF particles are too large for phagocytosis to occur and therefore the mechanisms of inflammatory responses are different compared with phagocytosable debris. The up-regulation of

TNF- $\alpha$  transcript level caused by SF may be related to the degradation products released from the SF particles. Surface-mediated effects, such as surface charge and shape, could cause further contribution to the inflammatory reactions. The amino acid residues with polar groups or positive charges on the surface of the SF protein may make them bind to the cells easier and then interact with the macrophages.

The data presented in this study demonstrate that SFS particles induced more significant macrophage activations characterized by TNF- $\alpha$  mRNA transcription than those observed during SFL stimulation. These results are likely due to the larger surface area–volume ratio inherent in SFS based on equal particle mass. This is in agreement with the previously published work which demonstrated that the total surface area or volume of the particles appeared to be an important factor in determining the inflammatory response during particle-induced cell activation.<sup>15,24</sup>

The inconsistency between transcription level of TNF- $\alpha$  mRNA and translation level of TNF- $\alpha$  may contribute to different efficiency of gene expression in different stimulated groups, inappropriate choice of testing time points, and the small sample size of the ELISA test. These limitations will remain unconfirmed until further experimentation can be performed under a better protocol design.

## CONCLUSION

SFS and SFL in culture with RAW 264.7 murine macrophage cells for 24 h can cause obvious up-regulation of TNF- $\alpha$  mRNA—observed to a higher degree in the SFS sample group—which indicated that both sizes of SF material could provoke inflammatory activity mediated by TNF- $\alpha$ . Despite the presence of precursory TNF- $\alpha$  mRNA, there was no statistically significant difference in the release of IL-1 $\beta$ , IL-6, or TNF- $\alpha$ , compared with the control group. These results indicated that SF particles of the tested dimensions may have limited inflammatory effect, thus suggesting good biocompatibility. Based on these findings, there seems to be a promising future for SF particle application in a variety of medical fields. However, further evaluation should be performed prior to any attempt at *in vivo* application of these particles.

## ACKNOWLEDGMENTS

The authors thank Yanping Zhang, Xinju Zhang, and Daquan Wu for technical help for real-time RT-PCR, they also thank Danny in University of Wisconsin School of Medicine for writing assistance.

## REFERENCES

1. Altman GH, Diaz F, Jakuba C, Calabro T, Horan RL, Chen J, Lu H, Richmond J, Kaplan DL. Silk-based biomaterials. *Biomaterials* 2003;24:401–416.
2. Wang Y, Kim HJ, Vunjak-Novakovic G, Kaplan DL. Stem cell-based tissue engineering with silk biomaterials. *Biomaterials* 2006;27:6064–6082.
3. Lu Q, Zhang B, Li M, Zuo B, Kaplan DL, Huang Y, Zhu H. Degradation mechanism and control of silk fibroin. *Biomacromolecules* 2011;12:1080–1086.

4. Hofmann S, Knecht S, Langer R, Kaplan DL, Vunjak-Novakovic G, Merkle HP, Meinel L. Cartilage-like tissue engineering using silk scaffolds and mesenchymal stem cells. *Tissue Eng* 2006;12: 2729–2738.
5. Lovett M, Cannizzaro C, Daheron L, Messmer B, Vunjak-Novakovic G, Kaplan DL. Silk fibroin microtubes for blood vessel engineering. *Biomaterials* 2007;28:5271–5279.
6. Kweon H, Lee KG, Chae CH, Balázs C, Min SK, Kim JY, Choi JY, Kim SG. Development of nano-hydroxyapatite graft with silk fibroin scaffold as a new bone substitute. *J Oral Maxillofac Surg* 2011;69:1578–1586.
7. Ghaznavi AM, Kokai LE, Lovett ML, Kaplan DL, Marra KG. Silk fibroin conduits: a cellular and functional assessment of peripheral nerve repair. *Ann Plast Surg* 2011;66:273–279.
8. Talukdar S, Nguyen QT, Chen AC, Sah RL, Kundu SC. Effect of initial cell seeding density on 3D-engineered silk fibroin scaffolds for articular cartilage tissue engineering. *Biomaterials* 2011;32: 8927–8937.
9. Wenk E, Wandrey AJ, Merkle HP, Meinel L. Silk fibroin spheres as a platform for controlled drug delivery. *J Controlled Release* 2008; 132:26–34.
10. Lammel AS, Hu X, Park SH, Kaplan DL, Scheibel TR. Controlling silk fibroin particle features for drug delivery. *Biomaterials* 2010; 31:4583–4591.
11. Kundu J, Chung YI, Kim YH, Tae G, Kundu SC. Silk fibroin nanoparticles for cellular uptake and control release. *Int J Pharm* 2010; 388:242–250.
12. Bessa PC, Balmayor ER, Azevedo HS, Nürnberger S, Casal M, van Griensven M, Reis RL, Redl H. Silk fibroin microparticles as carriers for delivery of human recombinant BMPs. Physical characterization and drug release. *J Tissue Eng Regen M* 2010;4: 349–355.
13. Goodman SB, Fornasier VL, Kei J. The effects of bulk versus particulate polymethylmethacrylate on bone. *Clin Orthop Relat Res* 1988;232:255–262.
14. Panilaitis B, Altman GH, Chen J, Jin HJ, Karageorgiou V, Kaplan DL. Macrophage responses to silk. *Biomaterials* 2003;24: 3079–3085.
15. Gelb H, Schumacher HR, Cuckler J, Ducheyne P, Baker DG. In vivo inflammatory response to polymethylmethacrylate particulate debris: effect of size, morphology, and surface area. *J Orthop Res* 1994;12:83–92.
16. Gonzalez O, Smith RL, Goodman SB. Effect of size, concentration, surface area, and volume of polymethylmethacrylate particles on human macrophages in vitro. *J Biomed Mater Res* 1996;30: 463–473.
17. Yang SY, Ren W, Park Y, Sieving A, Hsu S, Nasser S, et al. Diverse cellular and apoptotic responses to variant shapes of UHMWPE particles in a murine model of inflammation. *Biomaterials* 2002;23:3535–3543.
18. Zysk SP, Gebhard HH, Kalteis T, Schmitt-Sody M, Jansson V, Messmer K, Veihelmann A. Particles of all sizes provoke inflammatory responses in vivo. *Clin Orthopaed Relat Res* 2005;433: 258–264.
19. Eming SA, Krieg T, Davidson JM. Inflammation in wound repair: molecular and cellular mechanisms. *J Invest Dermatol* 2007;127: 514–525.
20. Caballero M, Bernal-Sprekelsen M, Calvo C, Farre X, Quinto L, Alos L. Polydimethylsiloxane versus polytetrafluoroethylene for vocal fold medialization: histologic evaluation in a rabbit model. *J Biomed Mater Res B Appl Biomater* 2003;67:666–674.
21. Chhetri DK, Jahan-Parwar B, Hart SD, Bhuta SM, Berke GS. Injection laryngoplasty with calcium hydroxylapatite gel implant in an *in vivo* canine model. *Ann Otol Rhinol Laryngol* 2004;113: 259–264.
22. Lim JY, Kim HS, Kim YH, Kim KM, Choi HS. PMMA (polymethylmethacrylate) microspheres and stabilized hyaluronic acid as an injection laryngoplasty material for the treatment of glottal insufficiency: *in vivo* canine study. *Eur Archiv Oto-Rhino-Laryngol* 2008;265:321–326.
23. Mishra PK, Wu W, Rozo C, Hallab NJ, Benevenia J, Gause WC. Micrometer-sized titanium particles can induce potent Th2-type responses through TLR4-independent pathways. *J Immunol* 2011; 187:6491–6498.
24. Jones LC, Frondoza C, Hungerford DS. Immunohistochemical evaluation of interface membranes from failed cemented and uncemented acetabular components. *J Biomed Mater Res* 1999; 48:889–898.
25. Catelas I, Petit A, Marchand R, Zukor DJ, Yahia L, Huk OL. Cytotoxicity and macrophage cytokine release induced by ceramic and polyethylene particles in vitro. *J Bone Joint Surg Br* 1999;81: 516–521.
26. da Silva RA, Leonardo MR, da Silva LA, Faccioli LH, de Medeiros AI. Effect of a calcium hydroxide-based paste associated to chlorhexidine on RAW 264.7 macrophage cell line culture. *Oral Surg Oral Med Oral Pathol Oral Radiol Endod* 2008;106:e44–e51.
27. Taira M, Kagiya T, Harada H, Sasaki M, Kimura S, Narushima T, Nezu T, Araki Y. Microscopic observations and inflammatory cytokine productions of human macrophage phagocytising submicron titanium particles. *J Mater Sci Mater Med* 2010;21:267–275.
28. Valles G, Gonzalez-Melendi P, Gonzalez-Carrasco JL, Saldana L, Sanchez-Sabate E, Munuera L, Vilaboa N. Differential inflammatory macrophage response to rutile and titanium particles. *Biomaterials* 2006;27:5199–5211.
29. Sargeant A, Goswami T. Pathophysiological aspects of hip implants. *J Surg Orthop Adv* 2006;15:111–112.
30. Hallab NJ, Jacobs JJ. Biologic effects of implant debris. *Bull NYU Hosp Jt Dis* 2009;67:182–188.
31. Ni Y, Zhao X, Zhou L, Shao Z, Yan W, Chen X, Cao Z, Xue Z, Jiang JJ. Radiologic and histologic characterization of silk fibroin as scaffold coating for rabbit tracheal defect repair. *Otolaryngol Head Neck Surg* 2008;139:256–261.
32. Cao ZB, Chen X, Yao JR, Huang L, Shao ZZ. The preparation of regenerated silk fibroin microspheres. *Soft Matter* 2007;3:910–915.
33. Hitchins VM, Merritt K. Decontaminating particles exposed to bacterial endotoxin (LPS). *J Biomed Mater Res* 1999;46:434–437.
34. Voronov I, Santerre JP, Hinek A, Callahan JW, Sandhu J, Boynton EL. Macrophage phagocytosis of polyethylene particulate in vitro. *J Biomed Mater Res* 1998;39:40–51.
35. Saxena RK, Vallyathan V, Lewis DM. Evidence for lipopolysaccharide-induced differentiation of RAW264.7 murine macrophage cell line into dendritic like cells. *J Biosci* 2003;28:129–134.
36. Rajanbabu V, Chen JY. The antimicrobial peptide, tilapia hepcidin 2-3, and PMA differentially regulate the protein kinase C isoforms, TNF-alpha and COX-2, in mouse RAW264.7 macrophages. *Peptides* 2011;32:333–341.
37. Rajanbabu V, Pan CY, Lee SC, Lin WJ, Lin CC, Li CL, Chen JY. Tilapia hepcidin 2-3 peptide modulates lipopolysaccharide-induced cytokines and inhibits tumor necrosis factor-alpha through cyclooxygenase-2 and phosphodiesterase 4D. *J Biol Chem*. 2010;285:30577–30586.
38. Byun EB, Sung NY, Kim JH, Choi JI, Matsui T, Byun MW, Lee JW. Enhancement of anti-tumor activity of gamma-irradiated silk fibroin via immunomodulatory effects. *Chem Biol Interact* 2010; 186:90–95.
39. Shive MS, Anderson JM. Biodegradation and biocompatibility of PLA and PLGA microspheres. *Adv Drug Deliv Rev* 1997;28:5–24.